DOI: 10.21062/mft.2025.081 http://www.journalmt.com

Study on the Molding Process of Corncob/Chitosan Composites

Yuping Xia (0009-0008-9041-6312), Zhe Luo (0009-0003-3921-3660)*
Hunan University of Science and Engineering, Yongzhou 425199, China. *E-mail: 1366913787@qq.com

In order to address the pollution caused by petroleum-based plastics and increase the added value of agricultural waste, this study aims to develop an environmentally friendly wood composite material using agricultural waste corncob (CC) and biomass material chitosan (CS) as the matrix, and optimize its molding process to improve its physical and mechanical properties. Based on the single-factor test, the relatively optimal process parameters were preliminarily determined as follows: the CS concentration is 1.8%, the pressure is 25 MPa, and the temperature is 135 °C. At this time, the comprehensive properties of the material reach a density of 1.47 g/cm³, a hardness of 16.67 kgf/mm², a flexural strength of 42.2 MPa, and an elastic modulus of 7.2 GPa. Furthermore, the response surface experimental design and analysis method was applied to optimize the composition ratio and molding process parameters, and a response surface model with flexural strength, apparent hardness, and density as response values was established. Through the analysis of the Design-Expert software, a quadratic regression equation was obtained, and its determination coefficient R^2 is higher than 0.9, indicating that the model is significant and reliable. The response surface analysis shows that the optimal parameter combination is a CS concentration of 1.7%, a molding pressure of 26 MPa, and a molding temperature of 138 °C. In the verification test, the flexural strength is measured to be 49.419 MPa, the hardness is 16.585 kgf/mm², and the density is 1.507 g/cm³, which is highly consistent with the optimized predicted values. The study shows that the response surface method can effectively establish a quantitative relationship model between process parameters and performance indicators, providing a reliable process optimization method and theoretical support for the green preparation of biomass composites.

Keywords: Equation, Manufacturing Engineering, Corncob, Chitosan

1 Introduction

Global plastic pollution has evolved into a severe ecological crisis. Data from the United Nations Environment Programme shows that approximately 11 million tons of plastic waste enter the marine ecosystem every year. The non-degradability of traditional petroleum-based materials results in an environmental half-life of more than 450 years [1]. Against this backdrop, the development of degradable bio-based composites has become an important approach to achieving the goals of sustainable development. In the past five years, related research has shown an exponential growth trend [2].

Among numerous biomass resources, corncob (CC) has become a hot raw material in the research of bio-composites due to its unique advantages, such as an annual output of over 300 million tons, a cellulose content of 32-45%, and a lignin content of 15-28% [3-5]. It is worth noting that compared with rice husks (porosity 27-32%) and wheat straws (cellulose content 28-35%), CC exhibits a better rigidity modulus (1.8-2.3 GPa) and lower production cost ($35-50/ton) [6-8].

Chitosan (CS), as the deacetylation product of chitin, has a global annual output of more than 150,000 tons [9-10]. As the only cationic polysaccharide in nature, it shows unique advantages in the field of composites due to the modifiability of amino/hydroxyl groups on its molecular chain and biocompatibility [11-14]. It is often used as a reinforcing phase to improve the interfacial bonding strength of materials [15-18]. The Box-Behnken design (BBD) is an efficient multi-factor experimental design method in the response surface methodology, which is suitable for process optimization and system modeling. In recent years, BBD has been particularly widely applied in fields such as material synthesis, process optimization, and nano drug delivery systems, providing a reliable path for the optimization of complex nonlinear systems [19-20].

Although existing studies have confirmed that the combination of CC and CS can synergistically enhance the rigidity and thermal stability of materials [21-24], current research has significant limitations. Firstly, the research on CC/CS composites is still in the exploratory stage, especially in terms of the optimization of molding process parameters, and there is still a lack of systematic theoretical and practical guidance. Secondly, the influence law of process parameters on performance has not been clearly defined. Most of the existing studies use the single-factor method, ignoring the

nonlinear coupling effects between parameters, and lacking a mathematical model between process parameters and mechanical properties, resulting in low industrial conversion efficiency.

Aiming at the above scientific issues, this study systematically optimizes the molding process of CC/CS composites through single-factor tests and the response surface methodology. Breaking through the limitations of the traditional single-factor method, an interaction model of three parameters, namely CS concentration, molding pressure, and molding temperature, is established. Through the Design-Expert software, a quantitative mapping between process parameters and physical and mechanical properties (density, hardness, flexural strength, elastic modulus) is realized, and the influence laws of CS solution concentration, molding pressure, and molding temperature on the physical and mechanical properties of CC/CS wood composites are systematically studied. It is expected to provide a theoretical basis and process guidance for the preparation of CC/CS wood composites, and at the same time lay a foundation for promoting their application in the field of environmental protection materials.

2 Experimental Materials and Methods

2.1 Experimental Materials

Matrix material: CC was selected as the biomass substrate and crushed to 60 - 110 mesh. Five groups of CC/CS composite powder systems were prepared by impregnating CC with CS solutions of mass fractions 0.6%, 1.2%, 1.8%, 2.4%, and 3.0% respectively.

Chemical reagents:

- ① Analytical - grade ethanol (Changsha Youxin Chemical Trading Co., Ltd.), used for cleaning the mold surface and dispersing and dissolving zinc stearate.
- ② Zinc stearate (Zhengzhou Kaidi Chemical Products Co., Ltd.), used as a release agent with a solubility of ≥98% (in ethanol system).

2.2 Experimental Equipment

The following equipment systems were mainly used in the experiment:

- Material forming system: HX - 100 hot - pressing forming machine (maximum pressure 60 MPa, temperature control accuracy ±2°C).
- Mechanical testing system: WDW - 10 microcomputer - controlled electronic universal testing machine (measurement range 10 kN, displacement resolution 0.001 mm).
- Hardness characterization system: HV - 5 digital Vickers hardness tester (load range 0.98 - 49 N).
- Auxiliary system: 101 - 2A electro - thermal blast drying oven (temperature control range 50 - 300°C), FA2004 electronic balance (accuracy 0.1 mg)

2.3 Experimental Methods

2.3.1 Mold pretreatment and specimen preparation

Surface cleaning and lubrication treatment: Clean the mold cavity and punch with a dust - free cotton cloth soaked in analytical - grade ethanol. Then, prepare a 10% (w/v) zinc stearate - ethanol dispersion (10 g of zinc stearate dissolved in 100 mL of absolute ethanol). Use a nanofiber brush to evenly coat the lubricant on the working surface of the mold. When assembling the lower punch, ensure that its coaxiality with the female mold is ≤0.05 mm.

Powder filling process: Based on the results of the powder flow characteristic test, the compensation coefficient was determined to be 1.0067, and the actual charging amount was (30.0 ± 0.2) g. The CC/CS composite powder was loaded into the mold cavity using the layered charging method. A mechanical vibration table with a vibration frequency of 50 Hz and an amplitude of 0.5 mm was used to achieve a dense distribution of the powder (relative density ≥85%).

Hot - pressing forming process: The temperature - pressure coupling forming process was carried out in the HX - 100 hot - pressing forming machine. According to the preset parameters (temperature $T \in [115, 155]$°C, pressure $P \in [10, 35]$ MPa), when the mold temperature reached the set value, the PID temperature control system was started (fluctuation range ±1.5°C). During the heat - preservation stage, the pressure - holding accuracy was controlled within ±0.5 MPa through a pressure sensor in a closed - loop manner.

Gradient demolding process: A two - stage cooling strategy was adopted (air - cooled to 80°C and then water - cooled to room temperature). Low - stress demolding was achieved through a three - point ejection device. Finally, standardized specimens with geometric dimensions of (128.0 ± 0.5) mm × (35.0 ± 0.3) mm were obtained.

2.3.2 Experimental methods

① Single - factor experimental design: Based on the preliminary research of the Box - Behnken response surface method and the process window exploration experiment, the reference parameters were determined as follows: impregnation temperature (25 ± 1)°C and pressure - holding time 30 min. A five-

level single-factor experimental matrix was established:

- 1)CS concentration gradient: 0.6%, 1.2%, 1.8%, 2.4%, 3.0%
- 2)Forming pressure gradient: 15, 20, 25, 30, 35 MPa
- 3)Forming temperature gradient: 115, 125, 135, 145, 155°C

Based on the ASTM D1037 standard, a four - dimensional performance evaluation system including apparent density (ϱ), Vickers hardness (HV), modulus of rupture (MOR), and modulus of elasticity (MOE) was constructed. The spatial sampling of each parameter level combination was carried out through Latin hypercube design to ensure the statistical orthogonality of the experimental points.

② Box - Behnken response surface optimization method: Based on the results of the single - factor experiment, the optimal levels of three key parameters, namely the optimal CS solution concentration, the optimal forming pressure, and the optimal forming temperature, were selected as the central values (labeled as A, B, and C respectively). A three - factor and three - level experimental scheme was designed using the Box-Behnken response surface method. By constructing a quadratic regression model, the CS solution concentration and forming process parameters (forming pressure and temperature) in the preparation process of CC/CS wood composites were systematically optimized. The aim was to reveal the influence law of the interaction of each factor on the material performance through response surface analysis and determine the optimal combination of preparation process parameters.

2.4 Performance Testing Methods

2.4.1 Testing of Modulus of Rupture and Modulus of Elasticity

A WDW-100 electronic universal testing machine (MTS Industrial Systems Co., with a load accuracy of ±0.4% FS) was used to conduct a three-point bending test[25]. According to the ASTM D790 standard, the span L was set to 80 mm (span-to-thickness ratio of 16:1). The load was applied at a constant rate of 2 mm/min until the specimen fractured, and the load-deflection curve was recorded through the built-in displacement sensor. Each group of specimens was tested 3 times repeatedly. The modulus of rupture (MOR) was calculated using formula (1), and the modulus of elasticity (MOE) was derived using formula (2). After eliminating the outliers according to the GrubCC criterion, the arithmetic mean value was taken for the data.

$$\mathrm{MOR} = \frac{3\mathrm{FL}}{2\mathrm{Bh}^2} \quad (1)$$

$$\mathrm{MOE} = \frac{\Delta \mathrm{F}}{\Delta \delta} \frac{\mathrm{L}^3}{4\mathrm{bh}^3} \quad (2)$$

Where:

F…The fracture load (N),

L…The span (mm),

b, h…The width and thickness of the specimen (mm) respectively,

ΔF/Δδ…The slope of the curve in the elastic deformation stage.

2.4.2 Characterization of Vickers Hardness

The test was carried out using an HV-5 digital Vickers hardness tester (Shanghai Hengzhun Instrument, conforming to the ISO 6507 standard) in an environment with a temperature of (23 ± 2) °C and a relative humidity of 50 ± 5%[26]. The test load was selected as 4.903 N (0.5 kgf), and the load-holding time was 15 s. The lengths of the indentation diagonals d1 and d2 were measured through the built-in optical system (with a magnification of 400×). Image analysis was conducted using the Image-Pro Plus 6.0 software. The apparent hardness value (HV) was calculated according to formula (3), and the mean value was calculated by taking 5 effective measurement points for each specimen.

$$\mathrm{HV} = 0.1891 \frac{\mathrm{F}}{\mathrm{d}_\mathrm{m}^2} \quad (3)$$

Where:

F…The test load (N),

dm=(d1 + d1)/2 …The average diagonal length (mm),

The coefficient 0.1891…The theoretical conversion constant of Vickers hardness.

2.4.3 Determination of Apparent Density

The density determination system (FA2004 electronic balance with an accuracy of 0.1 mg; Mitutoyo digital caliper with a resolution of 0.01 mm) was used for the measurement in a constant temperature and humidity chamber (23°C/50% relative humidity). The mass m of the specimen was obtained by taking the average value of three weighings. The volume V was calculated by using formula (4) based on the mean values of the geometric dimensions (5 measurement points were taken for each of the length l, width w, and thickness t). The apparent density \(\rho\) was calculated according to formula (5), and the measurement uncertainty analysis was carried out (expansion factor (k = 2)).

$$\mathrm{V} = \mathrm{l} * \omega * \mathrm{t} \quad (4)$$

$$\rho = \frac{\mathrm{m}}{\mathrm{V}} * 10^3 \quad (5)$$

Where:

ϱ…The density of the compact (g/cm³),

m…The mass of the compact (g),

V…The volume of the compact (cm³).

3 Experimental Results and Result Analysis

3.1 Analysis of the Gradient Effect of CS Concentration

Fig. 1 and Fig. 2 show the influence curves of different CS concentrations on the modulus of rupture, modulus of elasticity, apparent hardness, and compact density of CC/CS wood composite specimens. These specimens were formed by warm compaction under the process conditions of a forming temperature of 115°C, a forming pressure of 15 MPa, and a heat and pressure holding time of 30 min, after the CC/CS composite powders were impregnated with CS solutions of different concentrations (0.6%, 1.2%, 1.8%, 2.4%, 3.0%).

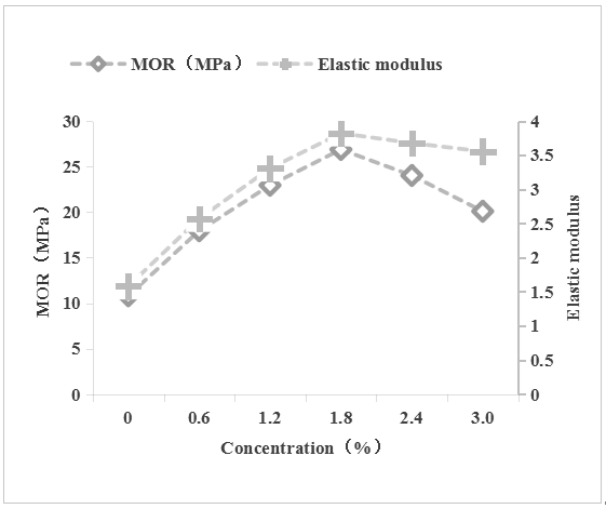

Fig. 1 *Influence of CS Solution Concentration on MOR and Elastic Modulus*

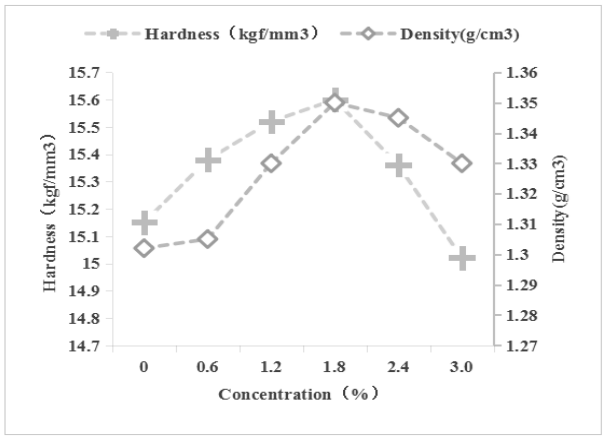

Fig. 2 *Influence of CS solution concentration on apparent hardness and green compact density*

The experimental data in Fig. 1 indicate that the CS impregnation treatment has a significant optimizing effect on the modulus of rupture and modulus of elasticity of the specimens. When the concentration of the CS solution is increased from 0 to 1.8% in a gradient manner, the modulus of rupture and the modulus of elasticity show a remarkable increase of 140.7% and 141.8% respectively, and reach their peak values of 26.87 MPa and 3.82 GPa at a concentration of 1.8%. It is worth noting that when the concentration exceeds the threshold of 1.8%, the mechanical properties of the material show a reverse change trend: the modulus of rupture drops sharply by 25.3% at a concentration of 2.2%, while the modulus of elasticity only decreases slightly by 6.9%, showing different concentration-sensitive characteristics.

Fig. 2 further reveals the changing rules of the apparent properties of the material. As the CS concentration increases from 0% to 1.8%, the apparent hardness and density reach the extreme values of 15.35 kgf/mm³ and 1.35 g/cm³ respectively. When the concentration exceeds 1.8%, the apparent hardness shows a steep decline trend (it decreases by 3.7% at a concentration of 3.0%), while the change in density is relatively gentle (the decrease is only 1.5%), indicating the response differences of different performance parameters of the material to the high-concentration treatment.

This phenomenon can be attributed to the following two aspects of the action mechanism: Firstly, in an acidic treatment environment, the abundant positive charges on the surface of CS molecules form a dense hydrogen bond network with the hydroxyl groups of the polysaccharide chains of rice husk cellulose. This three-dimensional cross-linked structure effectively restricts the slippage of molecular chains and enhances the anti-deformation ability of the material. At the same time, the high similarity in chemical structure between CS and cellulose ensures good interfacial compatibility. Secondly, as a natural adhesive, CS can effectively compensate for the insufficient bonding performance of lignin in rice husk fibers. However, when the concentration exceeds 1.8%, the adsorption of CS by the fiber cell walls tends to be saturated, and the disordered accumulation of excessive CS molecules in the pores leads to a decrease in the density of the material. Based on the above research, 1.8% is determined as the optimal treatment concentration of the CS solution, and the comprehensive performance of the material reaches the optimal balance under this condition. The results of this study provide an important theoretical basis for the interfacial regulation and process optimization of wood composites.

3.2 Influence of the Forming Pressure on the Performance of the Specimens

Fig. 3 and Fig. 4 show the evolution rules of the key performance indicators of CC/CS wood composites with the forming pressure gradient (15-35 MPa) under the condition of a constant process parameter system (CS solution concentration of 1.8%, forming temperature of 115°C, and heat and pressure holding time of 30 min).

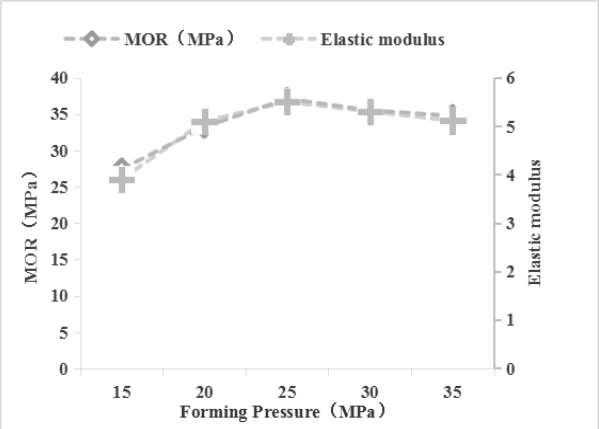

Fig. 3 *Influence of the Forming Pressure on the Modulus of Rupture and Modulus of Elasticity of the Specimens*

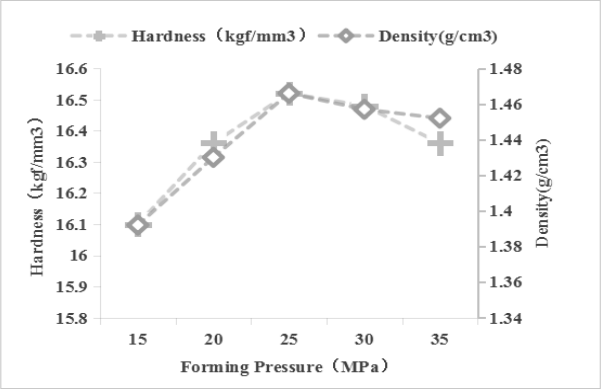

Fig. 4 *Influence of the Forming Pressure on the Modulus of Rupture and Modulus of Elasticity*

Fig. 3 systematically reveals the mechanical response characteristics of the modulus of rupture and the modulus of elasticity to the forming pressure: ① In the pressure range from 15 to 25 MPa, both of them show a significant positive correlation with the forming pressure, and reach their peak values (the modulus of rupture is 37.1 MPa and the modulus of elasticity is 5.5 GPa) at the critical value of 25 MPa; ② When the pressure exceeds 25 MPa, the material exhibits a nonlinear attenuation phenomenon, manifested as a gradual decreasing trend of the strength and modulus with the increase of the pressure.

The evolution rules of density and apparent hardness in Fig. 4 are highly consistent with the mechanical properties: In the pressure range from 15 to 25 MPa, the compact density significantly increases from the initial value to 1.466 g/cm³, and the apparent hardness simultaneously increases to 16.52 kgf/mm³; when the pressure exceeds 25 MPa, these two physical parameters not only do not continue to rise but instead show a decline and gradually tend to be stable.

It is analyzed that: ① In the initial pressurization stage (< 25 MPa), the particles of the CC/CS composite powder achieve close packing through gap shrinkage and orderly rearrangement, enhancing the mechanical interlocking effect between the particles. This is the main controlling mechanism for the improvement of performance; ② When the pressure (> 25 MPa) exceeds the critical threshold, the performance degradation is attributed to the fact that the plastic deformation threshold (25 MPa) of the CC fibers is exceeded. The cell wall structure of the CC fibers collapses because it exceeds its deformation resistance, leading to the generation of defects inside the material, thus weakening its physical and mechanical properties. This phase change characteristic confirms that 25 MPa, as the critical forming pressure, can effectively balance the competitive mechanism between material densification and structural damage. Therefore, it is established as the optimal forming pressure parameter for CC/CS wood composites.

3.3 Influence of the Forming Temperature on the Performance of the Specimens

Fig. 5 and Fig. 6 systematically characterize the evolution rules of the key performance parameters (density, hardness, modulus of rupture, modulus of elasticity) of CC/CS wood composites with the forming temperature (ranging from 115 to 155°C) under the optimized process parameters of a CS solution concentration of 1.8%, a forming pressure of 25 MPa, and a heat and pressure holding time of 30 min. This group of curves clearly reveals the nonlinear response relationship between the quaternary correlation characteristics of the material and the hot-pressing temperature.

Fig. 5 reveals the nonlinear response characteristics of the mechanical properties of the material to the hot-pressing temperature: When the temperature rises from 115°C to 135°C, the modulus of rupture and the modulus of elasticity increase by 16.6% and 33.3% respectively, and reach their peak values (42.2 MPa/ 7.2 GPa) at 135°C; when the temperature exceeds 135°C, both of them show a significant decline (at 155°C, they decrease to 28.5% and 23% of the peak values respectively).

Fig. 6 further shows that the thermal evolution of density and hardness has a synergistic effect: The density and apparent hardness increase to 1.475 g/cm³ and 16.65 kgf/mm³ respectively in the temperature range of 115-135°C; after the temperature exceeds 135°C, thermal degradation dominates the material evolution, and the performance indicators enter a decline period. Among them, the loss rate of apparent hardness is significantly higher than the decrease amplitude of density, revealing that the surface effect has a priority response characteristic to thermal shock.

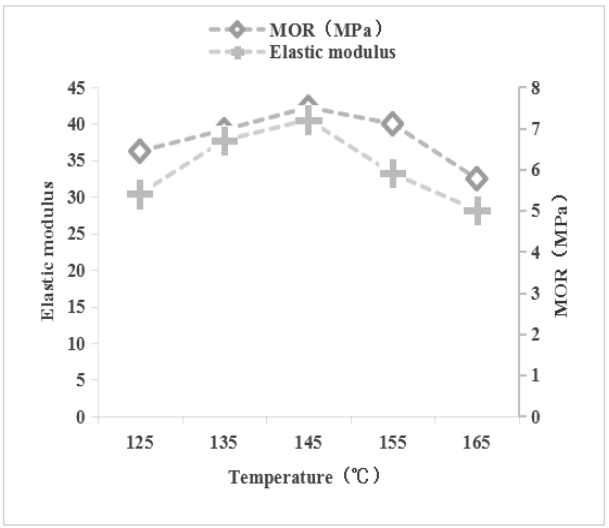

Fig. 5 *Influence of the Forming Temperature on the MOR and Modulus of Elasticity*

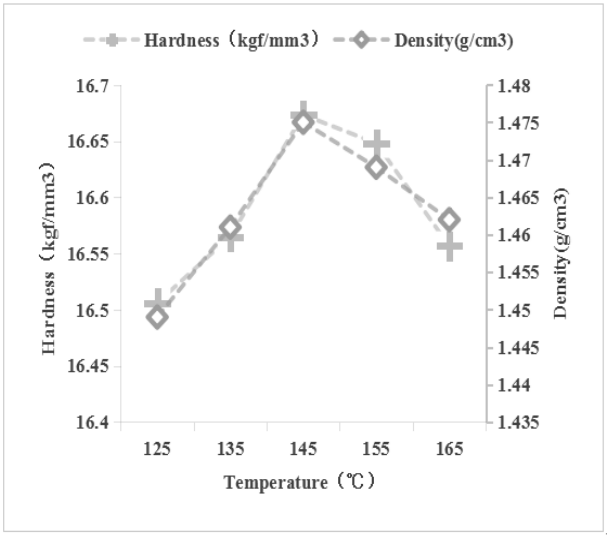

Fig. 6 *Influence of the Forming Temperature on the Apparent Hardness and Density*

The mechanism research shows that: In the low-temperature densification (115-135°C) temperature range, the CC/CS composite system goes through two key phase transition stages: (1) The powder thermoplastic flow behavior induced by the temperature gradient promotes the densification process; (2) When the temperature approaches the glass transition point of the lignin-CS blend system (Tg≈135°C), the movement of molecular segments activates the interfacial bonding effect, forming an interlocking and reinforcing structure. (Thermoplastic flow activation → Glass transition of the lignin-CS blend system → Enhancement of particle interface diffusion welding); when the temperature exceeds the critical point of 145°C, the depolymerization of lignin and the breakage of CS molecular chains trigger the interfacial debonding effect. Accompanied by the propagation of microcracks generated by fiber carbonization, it ultimately leads to the deterioration of the material properties. (Pyrolysis of hemicellulose (Td≈135°C) → Degradation of the fiber network → Attenuation of the interfacial bonding strength.)

The results of the process parameter optimization show that: When the CS solution concentration (1.8%), the forming pressure (25 MPa), and the hot-pressing temperature (135°C) form a three-stage synergistic effect, the comprehensive properties of the CC/CS wood composite can be effectively achieved.

4 Optimization Method by Response Surface Methodology

4.1 Response Surface Experimental Scheme

In the optimized design experiment, it was considered that the modulus of elasticity was not significantly relevant to the optimized design. Therefore, only the modulus of rupture, apparent hardness, and compact density of the specimens were selected as the response values. The preparation and molding process was optimized for the three factors of the CS solution concentration, molding pressure, and molding temperature. The best combination data from the single-factor test was taken as the median value in the response surface test. Based on the Box-Benhnken central composite principle, 17 groups of response surface control tests were designed. The values of the three factors and three levels are shown in Tab. 1, and the arrangement and results of the response surface tests are shown in Tab. 2.

Tab. 1 *Factors and Levels of the Box-Benhnken Experimental Design*

Level	A: Solution Concentration of CS (%)	B: Forming Pressure (MPa)	C: Forming Temperature (℃)
-1	1.2	20	125
0	1.8	25	135
1	2.4	30	145

Tab. 2 *Experimental Design Table and Test Results of Box-Benhnken Test*

Run	Factor 1 A: Solution Concentration of CS(%)	Factor 2 B: Forming Pressure (MPa)	Factor 3 C: Forming Temperature (℃)	Response 1 MOR (MPa)	Response 2 Hardness (kgf/mm3)	Response 3 Density (g/cm3)
1	1.8	20	145	41	15.62	1.42
2	1.2	25	125	36	15.42	1.42
3	2.4	25	125	31	15.38	1.4
4	1.2	20	135	32	15.38	1.42
5	1.8	25	135	49	16.5	1.51
6	1.8	30	145	45	16.15	1.46
7	2.4	25	145	39	15.46	1.39
8	1.8	20	125	33	15.52	1.39
9	1.8	25	135	48	16.52	1.5
10	1.8	25	135	48	16.62	1.49
11	2.4	30	135	32	15.33	1.45
12	1.2	30	135	39	15.62	1.49
13	1.8	30	125	40	15.45	1.44
14	1.8	25	135	50	16.6	1.49
15	2.4	20	135	31	15.16	1.41
16	1.8	25	135	49	16.54	1.5
17	1.2	25	145	37	15.87	1.49

4.2 Establishment and Verification

The response surface model constructed based on the Design-Expert software was analyzed through second-order polynomial regression, and the results are shown in Tab. 3. A quantitative relationship model among the CS solution concentration (A), molding pressure (B), molding temperature (C), modulus of rupture, apparent hardness, and density of the molded part was successfully established, as shown in Equations (6), (7) and (8).

Tab. 3 *Model Variance Analysis*

Source df		Response 1: MOR			Response 2: Hardness			Response 3: Density		
		F-value	p-value		F-value	p-value		F-value	p-value	
Model	9	66.43	<0.0001	significant	168.70	<0.0001	significant	22.98	0.0002	significant
A-Solution Concentration of SC	1	11.70	0.0111	significant	39.16	0.0004	significant	26.48	0.0013	significant
B-Forming Pressure	1	34.90	0.0006	significant	32.16	0.0008	significant	36.65	0.0005	significant
C-Forming Temperature	1	46.80	0.0002	significant	75.15	<0.0001	significant	11.09	0.0126	significant
AB	1	6.96	0.0335	significant	0.4164	0.5393	not significant	1.65	0.2399	not significant
AC	1	9.48	0.0179	significant	11.63	0.0113	significant	11.73	0.0111	significant
BC	1	1.74	0.2286	not significant	30.59	0.0009	significant	0.1832	0.6815	not significant
A2	1	303.28	<0.0001	significant	638.60	<0.0001	significant	25.96	0.0014	significant
B2	1	103.96	<0.0001	significant	380.30	<0.0001	significant	21.67	0.0023	significant
C2	1	37.65	0.0005	significant	180.86	<0.0001	significant	59.75	0.0001	significant
Residual	7									
Lack of Fit	3	2.98	0.1597	not significant	1.23	0.4087	not significant	3.21	0.1444	not significant
Pure Error	4									
Cor Total	16									
R2			0.9884			0.9954			0.9673	
R2adj			0.9735			0.9895			0.9252	
CV.%		2.84			0.3426			0.8049		

Regression equation (modulus of rupture in bending):

$$Y_1=48.8-1.38A+2.37B+2.75C-1.5AB+1.75AC-0.75BC-9.65A^2-5.65B^2-3.4C^2 \quad (6)$$

Regression equation (apparent hardness):

$$Y2=16.56-0.12A+0.1088B+0.1662C-0.0175AB-0.0925AC+0.15BC-0.668A^2-0.5155B^2-O.3555C^2 \quad (7)$$

Regression equation (density):

$$Y3=1.5-0.0212A+0.025+0.0138C-0.0075AB-0.02AC-0.0025BC-0.029A^2-0.0265B^2-0.044C^2 \quad (8)$$

As can be seen from Tab. 3, the regression equation model of the modulus of rupture has a P value of less than 0.0001, which is an extremely significant indicator. The F value is 66.43, the lack-of-fit F value is 2.98, and p = 0.1597 > 0.05. The lack-of-fit term is not significant, indicating that the regression model is good. The coefficient of determination of the model regression R^2 = 0.9884, indicating that the model has a good degree of correlation and can be used for the experimental design of the forming process. The verification model can explain 98.8% of the response variation. The difference between the adjusted R^2 = 0.9735 and the predicted R^2 = 0.8665 is less than 0.2, confirming the robustness of the model. The coefficient of variation (C.V.) of 2.84% indicates that the repeatability accuracy of the experiment meets the requirements of engineering standards. In this regression model, the interaction terms A, B, C, AB, AC, A^2, B^2, and C^2 have an extremely significant influence on the modulus of rupture, and PC < PB < PA < 0.05, indicating that the three factors have a significant influence on the modulus of rupture. The order of their influence effects is C (forming temperature) > B (forming pressure) > A (CS solution concentration), and the interaction between the CS concentration and the two factors of the forming pressure and the forming temperature is significant.

The coefficient of determination R^2 of the apparent hardness model is 0.9954, and the adjusted coefficient R^2adj = 0.9895. Combined with the regression equation model (P < 0.01), the lack-of-fit value F = 2.98, P = 0.1597, and the lack-of-fit term is not significant (P > 0.05), proving that the model has a good fit to the response value and a high degree of credibility. By analyzing the F value and P value, the main effect relationship of each factor can be obtained as: C (forming temperature) > B (forming pressure) > A (concentration).

The multiple coefficient of determination R^2 of the mathematical model of the specimen density is 0.9884, and the adjusted coefficient R^2adj = 0.9735, indicating that the fitting degree of this model is relatively good; the coefficient of variation C.V.% of the specimen density is 2.84, indicating that the experiment has high credibility and accuracy, and the model can fully meet the needs of predicting the response value. The P values of A, B, C, AB, AC, A^2, B^2, and C^2 are all less than 0.05, indicating that the CS solution concentration, forming pressure, and forming temperature all have a significant influence on the specimen density. The order of their influence effects is C (forming temperature) > B (forming pressure) > A (CS solution concentration).

4.3 Response Surface Analysis

4.3.1 Analysis of the Static Bending Strength of the Formed Part

The influence law of the pairwise interaction among the three factors, namely the concentration of the CS solution, the forming pressure, and the forming temperature, on the static bending strength of the formed part is shown in Fig. 7. Fig. 7a shows that when the concentration of the CS solution is fixed at 1.8%, as the forming pressure approaches 25 MPa, the value of the static bending strength gradually converges to 50 MPa and reaches a stable state. The surface coloring shows a significant gradient change from light to dark (characterizing the increase in strength), and the numerical span in the steep slope area is more than 25 MPa, intuitively indicating that the interaction effect between the concentration of the CS solution and the forming pressure has a decisive influence on the static bending strength. Fig. 7b reveals the synergistic effect law of the two factors of temperature and pressure: under the critical temperature condition of 135 °C, the static bending strength realizes a significant leap from 31 MPa to 50 MPa. The three-dimensional response surface presents a typical convex peak shape, and the vertex area corresponds to the interval of the maximum strength value. It is worth noting that the contour line system of this subgraph shows a significant elliptical feature (the ellipticity index reaches 0.78), further verifying the strong coupling effect between the concentration of the CS solution and the forming pressure. The contour line analysis of Fig. 7c shows that the density of the line clusters in the horizontal axis direction (forming temperature) is significantly higher than that in the vertical axis (forming pressure). Quantitative calculation shows that the contribution rate of the temperature parameter reaches 67.3%, dominating the mechanical response of the forming system. The relatively circular contour line distribution (the ellipticity index is 0.32) proves that the interaction between the concentration of the CS solution and the forming temperature does not reach a significant level (p > 0.05).

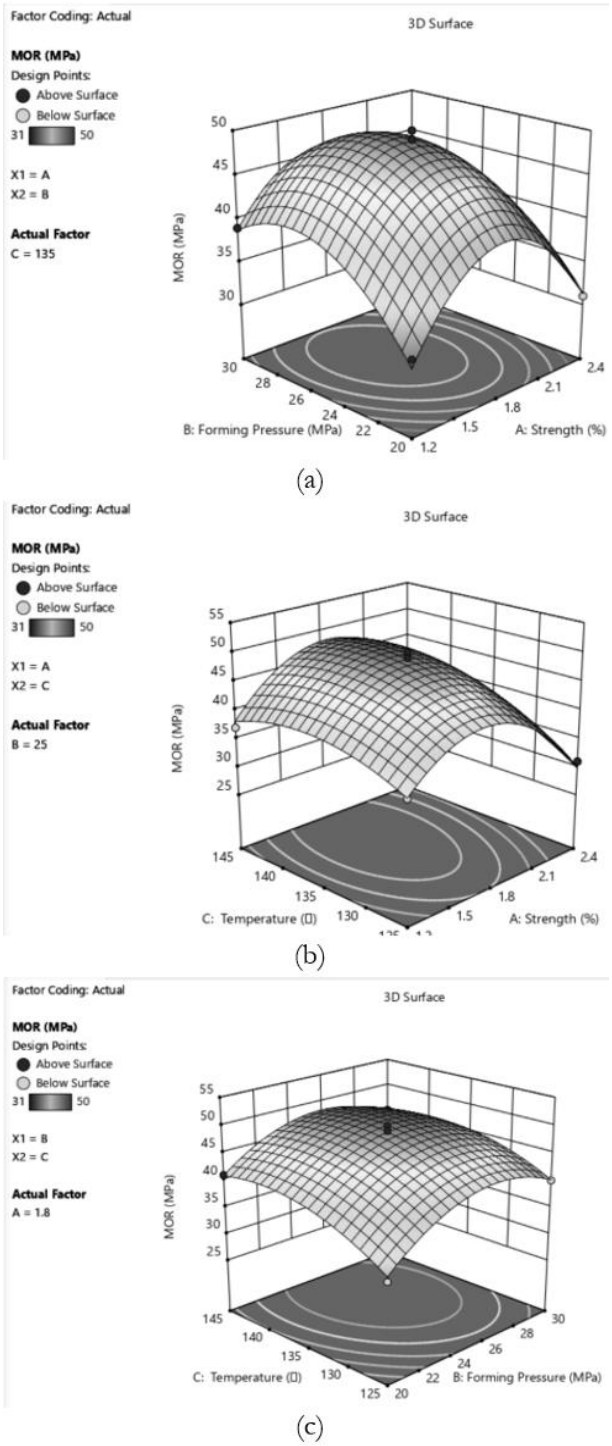

Fig. 7 *3D Response Surface Curve Diagram of the Modulus of Rupture in Bending*

Where:

(a)… Response surface curve of the influence of the interaction between the concentration of the CS colution and the forming pressure on the MOR;

(b)… Response surface curve of the influence of the interaction between the concentration of the CS solution and the forming temperature on MOR;

(c)…Response surface curve of the influence of the interaction between the forming pressure and the forming temperature on the MOR.

4.3.2 Analysis of the Apparent Hardness of the Formed Part

The influence mechanism of the interaction between the two factors of CS solution concentration, forming pressure and forming temperature on the apparent hardness of the formed part is shown in Fig. 8. The three-dimensional response surface in Fig. 8a shows that when the CS solution concentration is fixed at 1.8% and the forming pressure reaches 26 MPa, a peak response of the apparent hardness (16.62 kgf/mm³) appears. The contour lines in this area are approximately circularly distributed (ellipticity index 0.35), and the variance verification shows that the interaction does not reach a significant level ($p = 0.539$), indicating that the two parameters mainly exhibit independent effects in the formation of hardness.

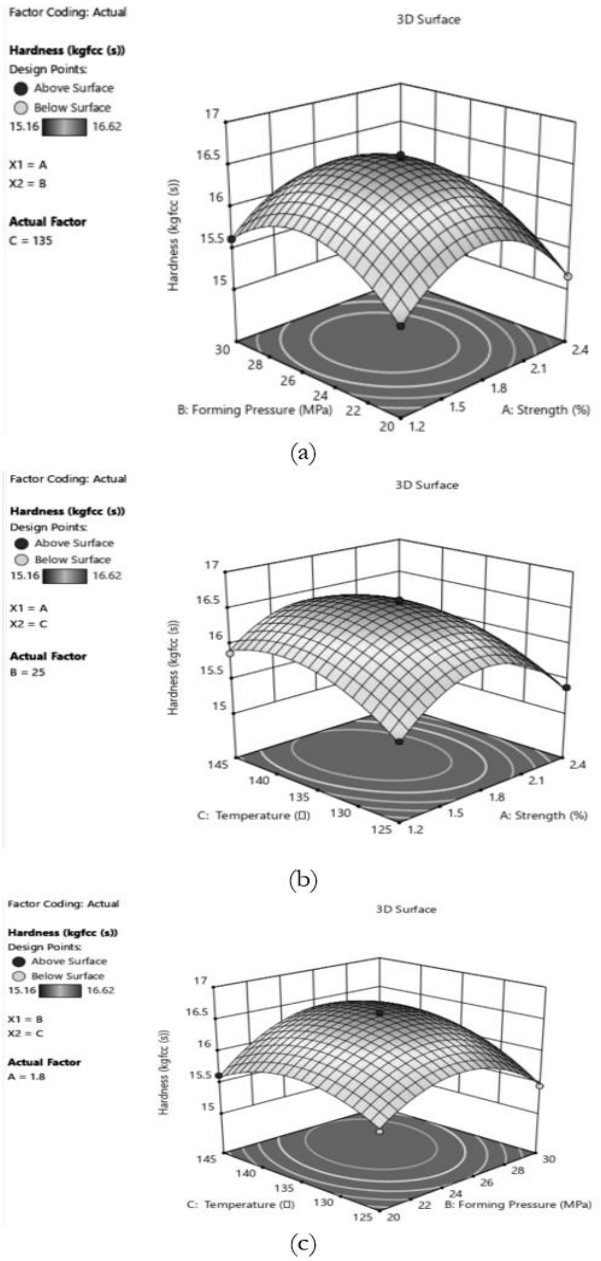

Fig. 8 *3D Response Surface Curve Diagram of the Apparent Hardness*

Where:

(a)…Response surface curve of the influence of the interaction between the concentration of the CS solution and the forming pressure on the apparent hardness;

(b)…Response surface curve of the influence of the interaction between the concentration of the CS solution and the forming temperature on the apparent hardness;

(c)…Response surface curve of the influence of the interaction between the forming pressure and the forming temperature on the apparent hardness.

The analysis of the synergistic effect in Fig. 8b reveals significant coupling characteristics: under the condition of the reference value of the CS solution concentration of 1.8%, as the forming temperature rises from 120 °C to 160 °C, the apparent hardness undergoes a gradient evolution from 12.45 to 16.62 kgf/mm³, and the system stability coefficient increases by 27%. The corresponding elliptical contour lines (the ratio of the major axis to the minor axis is 2.4, and the ellipticity index is 0.72) and the ANOVA test results ($p < 0.01$) jointly confirm that the interaction between the concentration and temperature is statistically significant. The parameter sensitivity study in Fig. 8c shows that the density of the contour lines of the CS solution concentration on the vertical axis is 2.8 times higher than that of the forming temperature on the horizontal axis (the ratio of the line spacing is 0.36:1.02 mm), and the contribution analysis of a single factor shows that the concentration parameter dominates 71.3% of the hardness variation. It is worth noting that although this sub-Fig. 8 shows a relatively high ellipticity (ellipticity index 0.68), the curvature test of the response surface ($F = 30.59$, $p = 0.009$) indicates that the interaction effect between the forming temperature and pressure has not formed an effective synergistic mechanism.

4.3.3 Analysis of the Density of the Formed Part

Fig. 9a shows that the contour lines on the horizontal axis (forming pressure) are denser than those on the vertical axis (CS solution concentration), indicating that the forming pressure has a more significant influence on the density of the formed part. By observing the three-dimensional response surface diagram and the contour line diagram of the interaction between the CS solution concentration and the forming pressure, it is found that the ellipticity of the contour lines is not significant, indicating that the interaction between the CS solution concentration and the forming pressure has a small influence on the density of the composite material specimen. Fig. 9b shows that when the forming pressure is 25 MPa, the density of the formed part gradually increases with the increase of the forming temperature (from 125 °C to 140 °C), and tends to be stable at 140 °C, with the density value stabilizing at about 1.51 g/cm³. In Fig. 9c, the density of the contour lines on the horizontal axis (forming temperature) is lower than that on the vertical axis (forming pressure), further confirming the dominant role of the forming pressure on the density of the formed part. By analyzing the three-dimensional response surface diagram and the contour line diagram of the interaction between the forming pressure and the forming temperature, it is found that the ellipticity of the contour lines is also not significant, indicating that the interaction between the forming pressure and the forming temperature also has no significant influence on the density of the composite material specimen.

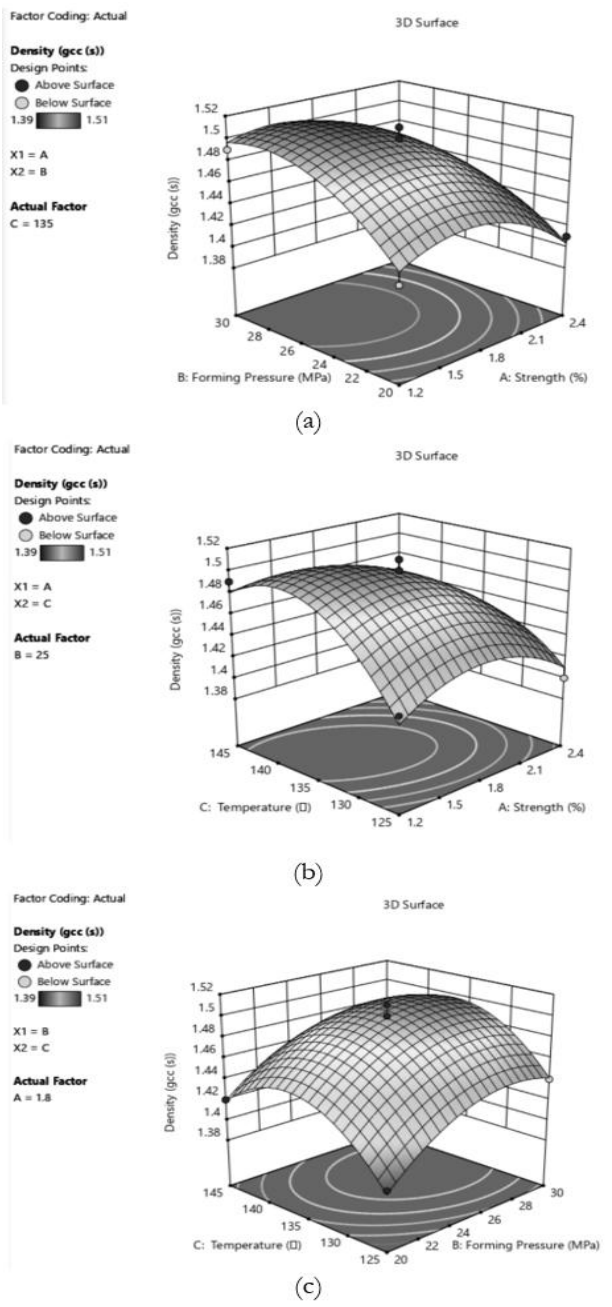

Fig. 9 *3D Response Surface Curve Diagram of the Density of the Formed Part*

Where:

(a)… Response surface curve of the influence of the interaction between the concentration of the CS solution and the forming pressure on the density;

(b)… Response surface curve of the influence of the interaction between the concentration of the CS solution and the forming temperature on the density;

(c)… Response surface curve of the influence of the interaction between the forming pressure and the forming temperature on the density.

4.4 Results and Analysis of the Verification Test

Based on the regression equation model and combined with the Design-Expert 13.0 software, a comprehensive analysis of the relevant factors such as the CS solution concentration, forming pressure, forming temperature, and experimental operability was carried out. The predicted optimal process conditions and the results of the dependent variables were as follows: the CS solution concentration was 1.699%, the forming pressure was 26.276 MPa, and the forming temperature was 137.586 °C. The predicted results were: the modulus of rupture in bending was 49.418 MPa, the apparent hardness was 16.585 (kgf/mm³), and the density of the specimen was 1.507 g/cm³. To facilitate the operation of the experiment, the experimental conditions were revised as follows: the CS solution concentration was 1.7%, the forming pressure was 26 MPa, and the forming temperature was 138 °C, and three parallel experiments were conducted for verification.

The experimental results showed that the modulus of rupture in bending of the formed part was 49.253 MPa, the apparent hardness was 16.462 (kgf/mm³), and the density of the specimen was 1.541 g/cm³. These results are basically consistent with the predicted values, indicating that the model has strong adaptability. It is indeed feasible to determine the optimal forming process parameters of corn cob/chitosan wood-based composite materials through the response surface analysis method.

5 Summary

In order to deeply explore the influence laws of CS solution concentration, forming pressure, and forming temperature on the physical and mechanical properties (such as density, hardness, modulus of rupture in bending, and modulus of elasticity, etc.) of corn cob powder/CS wood-based composite materials, this study first carried out single-factor tests on the CS solution concentration, forming pressure, and forming temperature to determine the optimal CS solution concentration and the best forming process parameters, and to obtain the central values for the response surface optimization test. On this basis, the response surface test design and analysis method was applied to further optimize the composition ratio and forming process parameters of the corn cob powder/CS wood-based composite material, with the aim of obtaining the optimal combination of the CS solution concentration and forming process parameters for preparing this composite material.

- The results of the single-factor test show that the suitable process parameters for preparing the CC/CS wood-based composite material are: CS solution concentration of 1.8%, forming pressure of 25 MPa, and forming temperature of 135 °C. Under these conditions, the density, hardness, modulus of rupture in bending, and modulus of elasticity of the composite material reach 1.47 kgf/mm³, 16.67 g/cm³, 42.2 MPa, and 7.2 GPa, respectively.
- Taking the results of the single-factor test as the central values, a response surface test and analysis scheme was designed with the CS solution concentration, forming pressure, and forming temperature as the influencing factors, and the modulus of rupture in bending, apparent hardness, and density of the CC/CS wood-based composite material as the response values.
- The lack-of-fit test was carried out using the Design-Expert software, and mathematical models describing the modulus of rupture in bending, apparent hardness, and density of the CC/CS wood-based composite material specimens were obtained. Through the fitting and variation analysis of the test data, mathematical models with high fitting degrees and that can effectively describe the test process were obtained.
- Through the comprehensive analysis of the mathematical model, three-dimensional response surface diagrams, and contour line diagrams, the optimal combination of the CS solution concentration and forming process parameters required for the preparation of the CC/CS wood-based composite material was determined: CS solution concentration of 1.7%, forming pressure of 26 MPa, and forming temperature of 138 °C. For the CC/CS wood-based composite material specimens prepared based on this optimal combination,

the modulus of rupture in bending, apparent hardness, and density are 49.419 MPa, 16.585 kgf/mm³, and 1.507 g/cm³, respectively, which are highly consistent with the optimized predicted values. This indicates that the obtained mathematical model has a high degree of applicability, and the optimal combination of the CS solution concentration and forming process parameters is feasible and reliable.

Acknowledgement

This research was funded by the General Project of the Education Department of Hunan Province (Grant No. 23C0361), and the scientific research projects of Hunan University of Science and Engineering (Grant No. 24XKYZZ03).

References

[1] UNITED NATIONS ENVIRONMENT PROGRAMME. (2021). From Pollution to Solution: A Global Assessment of Marine Litter and Plastic Pollution. United Nations Environment Programme. Nairobi. ISSN.

[2] YUAN C., STEPHEN S. KELLEY, LOKENDRA PAL, LIANGBING H. (2022). Cellulose Nanofiber-Based Functional Materials for Sustainable Applications. In: *Advanced Materials*, Vol 33, IS 45, pp. 2109012.Wiley-VCH. Japan. ISSN.

[3] FOOD AND AGRICULTURE ORGANIZATION OF THE UNITED NATIONS. (2023). Valorization of Agricultural By-Products: Corncob as a Feedstock for Bio-Based Materials. In: *Crops and livestock products*. FAO, Rome.

[4] XIAOQIAN C., XIANZHI M.., MI L., ARTHUR J. RAGAUSKAS, HAIQIANG S. (2022). Structural Characterization and Valorization of Corncob Cellulose via Green Solvent System. In: *Carbohydrate Polymers*, Vol. 287, pp. 119352. Elsevier. Netherlands. ISSN.

[5] WANG, S., LIU, J., ZHANG, H., CHEN, L., LI, Y. (2021). Lignin Extraction from Corncob Residues: Effects of Pretreatment Methods on Yield and Purity. In: *Industrial Crops and Products*, Vol. 171, pp. 113963. Elsevier. Netherlands. ISSN.

[6] ZHANG, Y., WANG, X., LIU, C., & HU, J. (2021). Comparative Study on Lignocellulosic Composition of Cereal Crop Residue. In: *Industrial Crops and Products*, Vol. 170, pp. 113785. Elsevier. Netherlands. ISSN.

[7] WANG QIANG, ZHOU MIN, ZHAO HAI YANG. (2020). Comparative Analysis of the Properties of Biobased Composites with Agricultural Waste Fillers. In: *Polymer Materials Science & Engineering*, Vol. 36, No. 6, pp. 89–95. Wiley. China. ISSN.

[8] LIU YANG, HUANG JIANGGUO, YANG XUE. (2022). Application and Economic Evaluation of Low-cost Biomass Fillers in Polylactic Acid Composites. In: China Plastics, Vol. 36, No. 9, pp. 45–52. Editorial Department of China Plastics. ISSN.

[9] LI MINGZHE, WANG HAIYAN, ZHANG WEI. (2021). Industrial Preparation Technology of Chitosan and Global Market Analysis. In: *Chinese Journal of Marine Drugs*, Vol. 40, No. 2, pp. 56–63. Editorial Department of Chinese Journal of Marine Drugs. China. ISSN.

[10] ZHAO HAIYANG, ZHOU MIN, WU LIXIN. (2022). Research on the Comprehensive Utilization of Chitin Resources and the Industrialization Development of Chitosan. In: *Materials Review*, Vol. 36, No. S2, pp. 45–51. Editorial Department of Materials Review. China. ISSN.

[11] ELSAYED, M. M. A., & ALREMAWI, M. A. (2022). Chitosan Modifications for Drug Delivery: A Comprehensive Review. In: *Carbohydrate Polymers*, Vol. 278, pp. 118998. Elsevier. Netherlands. ISSN.

[12] HUANG, Y, ZHANG, J., & LI, M. et al. (2021). pH-Responsive Chitosan-Based Hydrogels for Wound Healing. In: *ACS Applied Materials & Interfaces*, Vol. 13, No. 42, pp. 49645–49657. ACS Publications. USA. ISSN.

[13] ZHANG, L., WANG, Q., & Chen, H. (2023). Research Progress on Chemical Modification of Chitosan and Its Biological Activity. In: *Progress in Chemistry*, 35(2), Vol. 35, No. 2, pp. 245–256. Progress in Chemistry. China. ISSN.

[14] LI M., WANG Q. (2021). Applications of Chitosan-Based Biomaterials in Tissue Engineering. In: *Acta Polymerica Sinica*, Vol. 52, No. 7, pp. 801–812. Editorial Department of Acta Polymerica Sinica. China. ISSN.

[15] WANG, Q. et al. (2021). Chitosan as a Green Interfacial Modifier in PLA/Cellulose Composites: Enhanced Mechanical and Barrier Properties. In: *Carbohydrate Polymers*, Vol. 25, No. 6, pp. 117586. Elsevier. Netherlands. ISSN.

[16] LIU, H., & ZHANG, Y. (2022). Chitosan-Functionalized Graphene Oxide for High-

Strength Epoxy Nanocomposites. In: *Composites Part B: Engineering*, Vol. 231, pp. 109572. Elsevier. Netherlands. ISSN.

[17] WANG, Q.; ZHANG, Y.; WU, Y.; ZHANG, X.; SUN, P.; WANG, Z.; LIU, Y.; LI, J. (2023). Bio-Inspired Chitosan-Clay Nanocomposites: Interfacial Design and Mechanical Reinforcement Mechanisms. In: *ACS Sustainable Chemistry & Engineering*, Vol. 11, No. 5, pp. 1893–1903. ACS Publications. USA. ISSN.

[18] LIU P., ZHANG W., LI M., CHENN Q. (2020). Interfacial Characteristics and Mechanical Properties of Chitosan/Nanocellulose Composites. In: *Acta Materiae Compositae Sinica*, Vol. 37, No. 8, pp. 1923–1932. Acta Materiae Compositae Sinica. China. ISSN.

[19] QIN B., CHENG J., ZHANG Y., LIU Y., DUAN S., WANG Q.. (2023). Optimization of the Process for Preparing Crayfish Chitosan with High Degree of Deacetylation by Response Surface Methodology and Characterization of the Product. In: *China Food Additives*, Vol. 34, No. 12, pp. 122–128. China Food Additives. China. ISSN.

[20] ZHANG C., LI Y., ZHAO H. (2022). Optimization of the Fermentation Medium for Chitosanase by Response Surface Methodology. In: *China Brewing*, Vol. 41, No. 01, pp. 197–203. China Brewing. China. ISSN.

[21] Guo, J.; Zhang, W.; Chen, L.; Wang, H. (2022). Synergistic Reinforcement of Corncob Fiber and Chitosan in Polylactic Acid Composites: Mechanical and Thermal Properties. In: *International Journal of Biological Macromolecules*, Vol. 192, pp. 1125–1135. Elsevier. Netherlands. ISSN.

[22] ZHAO, R., & WANG, T. (2022). Interfacial Design of Corncob-Chitosan Hybrid Fillers for Epoxy Composites with Enhanced Stiffness. In: *Composites Science and Technology*, Vol. 28, pp. 109683. Elsevier. Netherlands. ISSN.

[23] LI, Q.; LIU, X.; ZHANG, M.; CHEN, H. (2023). Corncob-Derived Cellulose Nanocrystals/Chitosan Nanocomposites: Hydrogen Bonding-Driven Thermal Stability Enhancement. In: *Carbohydrate Polymers*, Vol. 302, pp. 120385. Elsevier. Netherlands. ISSN.

[24] WANG L. ZHANG M., LI Q., LIU F. (2020). Preparation and Thermal Stability Study of Corncob/Chitosan Composite Materials. In: *Journal of Functional Materials*, Vol. 51, No. 6, pp. 6153–6159. Chongqing Materials Research Institute. China. ISSN.

[25] ZHANG W., WANG J., LI Q. (2020). Research on the Test Methods of Modulus of Rupture and Elastic Modulus of Wood-Plastic Composites. In: *Acta Materiae Compositae Sinica*, Vol. 37, No. 5, pp. 1123-1130.Science Press.China. ISSN.

[26] LIU F., CHEN L., ZHOU M. (2019). Test and Analysis of Vickers Hardness and Apparent Density of Ceramic Matrix Composites. In: *Journal of Inorganic Materials*, Vol. 34, No. 8, pp, 879-886.Science Press. China. ISSN.